Wu Elimination Method Applied in Static Analysis of the Power System

QING ZHANG, and CHEN CHEN
Department of Electrical Engineering
Shanghai Jiao Tong University
800 Dong Chuan Road, Shanghai 200240
CHINA
chchen@sjtu.edu.cn http://www.sjtu.edu.cn

Abstract: - Wu Elimination Method is applied to obtain analytical solution of power flow equations without either extraneous roots or missing roots. The symbolic process of Wu Elimination is implemented by software MAPLE. A minor group of solutions is obtained under low load other than the major group of solutions. Based on computation, analytical $V-P$, $V-Q$ curves as well as the steady state operation area. The results are compared with the results of Homotopy Method. Discussion on unstable equilibrium points is presented which is potentially valuable for research on voltage stability and angle stability of complex power systems.

Key-Words: - Wu Elimination Method, Power system, $V-P$ curve, Voltage stability, Angle stability

1 Introduction

Wu Elimination Method (WEM) is proposed to solve simultaneous polynomial equations, and provide efficient algorithm to calculate not only with numbers but also with symbols. So far, WEM, also called the mechanized mathematics, has already been applied in the proof of theorems by machine in many theoretic aspects (mathematics, physics, etc.). WEM is able to enumerate all the solutions of polynomial equations without either extraneous or missing roots. The solutions are analytical and superior to numerical methods. Papers [1],[2] were on WEM applied in power system, and others in constrained dynamics [3] and in rotor dynamics [4]. This paper presents WEM applied in solving power flow equations.

Newton-Ralfson method [5] and fast decoupled method [6], etc. are well known in solving power flow equations. Those numerical methods depend on the initial conditions and are not possible to obtain the unstable parts since the Jacobian matrix does not converge under those conditions. Power flow equations which are nonlinear exhibit multiple solutions [7]-[9]. Homotopy method was employed in [9]-[11] and genetic algorithms was applied in [12] to obtain all the possible solutions. An iteration method was newly proposed in [13] for low-voltage power flow solution. WEM can obtain all the solutions to simultaneous nonlinear equations, so as solutions to the power flow equations.

Voltage stability is the most widespread power quality issue. Research on propagation of voltage fluctuation along practical power distribution systems is presented in [14].Continuation power flow is used in static voltage stability [15]. A novel approach is applied to determine the Hopf bifurcation point of dynamic voltage stability [16]. On basis of results obtained by WEM, the $V-P$ is discussed, and the voltage stability is analyzed in this paper.

2 Basic Concept of WEM

The basic concept of WEM is presented in this section. Comparison between WEM and Gaussian Elimination Method is discussed for clear comprehension of WEM. Furthermore, the process to apply WEM is given in this section.

2.1 Wu Elimination Method and Gaussian Elimination Method

Gaussian Elimination method is well known in solving linear equations. A set of triangular equations is obtained by elimination and equivalent to the original equation set. Then the triangular equation set is easy to be solved by simple substitution. The Wu Elimination is implemented by addition or subtraction of polynomials, after the process a set of triangular equations is obtained. The format of the triangular polynomial equation set is as follows:

$$\begin{cases} P_1(x_1,u_1,u_2\ldots u_{n-r})=0 \\ P_2(x_1,x_2,u_1,u_2\ldots u_{n-r})=0 \\ \quad\cdots \\ P_r(x_1,x_2\ldots x_r,u_1,u_2\ldots u_{n-r})=0. \end{cases} \tag{1}$$

where u_1, u_2, $\cdots$, u_{n-r} are all the parameter variables in the polynomials above.

Wu Elimination intends to reduce the number of

parameters similar to Gaussian Elimination. However, the set of triangular equations is not exactly equivalent to the original set of equations during Wu Elimination which is different from the Gaussian Elimination. The solutions of the set of original equations are the solutions of the set of triangular equations, but not necessarily vice versa. The Wu Elimination is implemented by calculating the remainder of polynomials.

2.2 Calculation of Characteristic Set in Wu Elimination

The kernel of WEM is calculating the characteristic set (CS). The process of calculating the CS is actually the process to eliminate the variables.

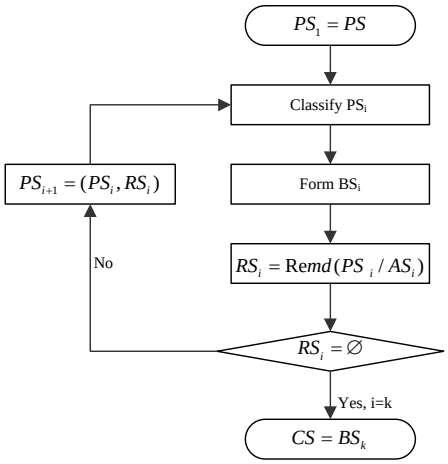

Fig. 1 Flow chart of calculation of characteristic set.

The procedure is composed by finite repeats of the steps as follows [17]:

$PS = \{P_1, P_2 \cdots P_k\}$ is denoted as PS_1 .

In i^{th} round of elimination, the operation on PS_i is as follows:

Step 1: Classify the polynomials in PS_i by class which is determined by the variables in the polynomials. Polynomials with the same class are in the same group.

Step 2: Form the basic set (BS_i). Select the polynomial with the lowest order exponent of the main variable in each group to form a triangular set and then transform the set into an ascending set.

Step 3: Calculate the remainder set (RS_i) of PS_i about BS_i , which is denoted by $RS = \mathrm{Re}md(PS / BS)$. Then put RS_i into PS_i to get PS_{i+1} . That means $PS_{i+1} = (PS_i, RS_i)$.

If $RS_i = \varnothing$, which means the remainders of PS_i about BS_i are zeroes, then BS_i is the characteristic set of PS , denoted by CS ; Otherwise, continue to repeat the steps above.

The process of elimination is described by the flow chart in Fig. 1.

3 WEM Applied in Solving Power Flow Equations

A power system contains $n+1$ nodes, of which n_s are PV nodes, $n-n_s$ are PQ nodes and one is the slack node. The power flow equations are denoted in Cartesian coordination. The voltage of i^{th} node is denoted as $V_i = e_i + jf_i$ $(j = \sqrt{-1})$. All the power flow equations are in 2^{nd} order as follows:

PQ node:

$$P_{is} - e_i \sum_{k=1}^{n+1}(G_{ik}e_k - B_{ik}f_k) - f_i \sum_{k=1}^{n+1}(G_{ik}f_k + B_{ik}e_k) = 0 \quad (2a)$$

$$Q_{is} - f_i \sum_{k=1}^{n+1}(G_{ik}e_k - B_{ik}f_k) + e_i \sum_{k=1}^{n+1}(G_{ik}f_k + B_{ik}e_k) = 0, \quad (2b)$$

where $i = 1, 2, \cdots n - n_s$.

PV node:

$$P_{is} - e_i \sum_{k=1}^{n+1}(G_{ik}e_k - B_{ik}f_k) - f_i \sum_{k=1}^{n+1}(G_{ik}f_k + B_{ik}e_k) = 0 \quad (3a)$$

$$V_{is}^{\ 2} - (e_i^{\ 2} + f_i^{\ 2}) = 0, \quad (3b)$$

where $i = n - n_s + 1, n - n_s + 2, \cdots n$, G_{ik} and B_{ik} are the real part and imaginary part of i^{th} node's admittance respectively. The power injection at PQ node i is denoted as $S_{is} = P_{is} + jQ_{is}$, in which P_{is} is the active power, Q_{is} is the reactive power. For PV node, the voltage magnitude is a constant, denoted by $V_{is}\angle\theta$ and the active power injection is denoted by P_{is} .

The procedure of applying WEM in solving power flow equations is a process to solve the CS of the power flow equations. According to the calculation flow chart, power flow equations should be classified according to the class. For a power system with $n+1$ nodes, there are $2n$ power flow equations containing variables which are denoted by $(e_1, f_1, e_2, f_2, \cdots e_n, f_n)$. For convenience, suppose the sequence of eliminating variables is $(e_1, f_1, e_2, f_2, \cdots e_n, f_n)$, then all the power flow equations are classified into $2r$ groups according to the class of each equation.

The polynomial series is denoted by $PS = \{P_1, P_2, \cdots P_{n_1}; P_{n_1+1}, \cdots P_{n_1+n_2}; \cdots; P_{n_1+n_2+\cdots+n_{r-1}+1}, \cdots P_{n_1+n_2+\cdots+n_{2r}}\}$, where

$$\begin{cases} CLS(P_1) = \cdots = CLS(P_{n_1}) = 2n - 2r \\ CLS(P_{n_1+1}) = \cdots = CLS(P_{n_1+n_2}) = 2n - 2r + 1 \\ \quad \cdots \\ CLS(P_{n_1+n_2+\cdots+n_{2r-2}+1}) = \cdots = CLS(P_{n_1+n_2+\cdots+n_{2r-1}}) = 2n - 1 \\ CLS(P_{n_1+n_2+\cdots+n_{2r-1}+1}) = \cdots = CLS(P_{n_1+n_2+\cdots+n_{2r}}) = 2n, \end{cases} \quad (4)$$

$n_1 + n_2 + \cdots + n_{2r} = 2n.$

The main variable in the first group which contains n_1 polynomials is f_r. The main variable in the $2r^{th}$ group which contains n_{2r} polynomials is e_1.

According to the calculation flow in Figure 1, select a polynomial with the lowest power exponent of the main variable in the $2r$ groups respectively to form the BS_1 of PS after classifying all the equations, then solve the remainder set which is denoted by RS_1 of PS about BS_1, and then RS_1 together with PS is denoted by PS_2, which means $PS_2 = (PS, RS_1)$. Repeat the elimination operation until $RS_i = \varnothing$, that means the remainder of any polynomial in PS_i about BS_i is zero. At last, there are $2n$ polynomials in BS_i which is denoted as follows:

$$\begin{cases} B_1(f_n) = 0 \\ B_2(f_n, e_n) = 0 \\ \quad \cdots \\ B_{2n-1}(f_n, e_n, \ldots f_r, e_r, \ldots f_1) = 0 \\ B_{2n}(f_n, e_n, \ldots f_r, e_r, \ldots f_1, e_1) = 0 \end{cases} \quad (5)$$

BS_i is a set of triangular equations which is easy to solve. However, BS_i is not equivalent to the original set of equations PS. In order to obtain the true solutions of PS, it is necessary to deal with the solutions of BS_i according to the theorems in WEM. A three-node system below is an example used to explain the application of WEM specifically.

4 Case Study

Fig. 2 shows a three-node system [10], [18]. The power injection of each node and reactant of each branch are also showed in the figure. All the parameters are per unit value. Node 1 is a PQ node. The voltage of node 1 is unknown, denoted by $V_1 = e_1 + jf_1$. Node 2 is a PV node. The voltage of node 2 is denoted by $V_2 = e_2 + jf_2$. WEM is applied to solve the power flow equations of the system shown in Fig. 2.

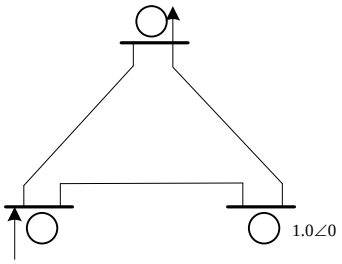

Fig. 2 Three-node system.

4.1 The calculation procedure

According to (2)-(3), four equations about e_1, f_1, e_2, f_2 are as follows:

$$\begin{cases} p_1 = -0.2 - 1.7214e_1^2 + 0.6807e_1e_2 + 2.5187e_1f_2 + 1.0407e_1 \\ \quad -1.7214f_1^2 + 0.6807f_1f - 2.5187f_1e_2 - 1.8552f_{12} \\ p_2 = -0.1 - 4.3739f_1^2 + 0.6807f_1e_2 + 2.5187f_1f_2 + 1.0407f_1 \\ \quad -4.3739e_1^2 - 0.6807e_1f_2 + 2.5187e_1e_2 + 1.8552e_1 \\ p_3 = -1.13430 + 0.6807e_1e_2 + 2.5187f_1e_2 \\ \quad +0.7536e_2 + 0.6807f_1f_2 - 2.5187e_1f_2 - 1.2351f_2 \\ p_4 = 1.00 - e_2^2 - f_2^2 \end{cases} \quad (6)$$

By calculation, the sequence of eliminating variable is f_1, f_2, e_1, e_2.The process of solving Eq. (6) by WEM is as follows: $CLS(p_1) = CLS(p_2) = CLS(p_3) = 4$, $CLS(p_4) = 3$. Select p_3 and p_4 to form basic set BS_1, and calculate the remainder set (R_{11}, R_{12}); Then $PS_2 = (p_1, p_2, p_3, p_4, R_{11}, R_{12})$. Select R_{12} and p_4 to form basic set BS_2, and calculate the remainder set of PS_2 about BS_2. Repeat the procedure to obtain the CS of (p_1, p_2, p_3, p_4). It is necessary to mention that the kernel of the procedure is forming the basic set. As mentioned before, polynomial with low power exponent of main variable is the first choice to form basic set. So it is unnecessary to do some calculation which would create remainder with very high power exponent of main variable.

The Table 1 below shows the process to calculate the CS of (6), in which PS_i has been classified into groups separated by parentheses.

The CS of (p_1, p_2, p_3, p_4) is $(R_{51}, R_{41}, R_{12}, p_3)$. According to WEM theorems, the zero set of the equations can be expressed by the formula $Zero(PS) = Zero(CS/I) + \sum Zero(PS, I_i)$ [17]. Under accurate calculation condition, the zero set is obtained by eliminate extra roots from zero set of CS. However, due to the complexity of power flow

equations and limit calculating ability of the software Maple, it is difficult to eliminate the extraneous roots under finite precision and the remainders of original equations on CS are not void.

In order to obtain the solutions of original equations, the following method is used in the paper: first obtain the solutions of the CS, and then back substitute the solutions into the original equations to calculate the errors. Extraneous roots are taken off by setting a certain error. Analysis of the results shows that the results obtained by WEM in the way are correct and highly precise.

Table 1
Solving CS of power flow equations of three-node system

	PS_i	BS_i	RS_i
1	$(p_1, p_2, p_3), (p_4)$	(p_4, p_3)	$R_{11} = \mathrm{Re}md(p_1 / BS_1)$
			$R_{12} = \mathrm{Re}md(p_2 / BS_2)$
2	$(p_1, p_2, p_3), (p_4, R_{11}, R_{12})$	(R_{12}, p_3)	$R_{21} = \mathrm{Re}md(p_4 / BS_2)$
			$R_{22} = \mathrm{Re}md(R_{11} / BS_2)$
3	$(p_1, p_2, p_3), (p_4, R_{11}, R_{12})$ (R_{21}, R_{22})	(R_{22}, R_{12}, p_3)	$R_{31} = \mathrm{Re}md(R_{21} / BS_3)$
4	$(p_1, p_2, p_3), (p_4, R_{11}, R_{12})$ (R_{21}, R_{22}, R_{31})	(R_{31}, R_{12}, p_3)	$R_{41} = \mathrm{Re}md(R_{22} / BS_4)$
5	$(p_1, p_2, p_3), (p_4, R_{11}, R_{12})$ $(R_{21}, R_{22}, R_{31}, R_{41})$	(R_{41}, R_{12}, p_3)	$R_{51} = \mathrm{Re}md(R_{41} / BS_5)$

Table 2
Solutions of three-node system by WEM

	e_1	f_1	e_2	f_2
1	0.031676	-0.041021	0.923984	-0.382430
2	0.967058	0.012746	0.996533	0.083196
3	-0.005182	-0.238396	-0.489061	-0.872249
4	-0.009146	-0.107354	-0.238492	-0.971144
5	0.187180+j0.849019	0.823769+j0.177733	-1.010476+j0.066342	-0.243358-j0.275469
6	0.187180-j0.849019	0.823769-j0.177733	-1.010476-j0.066342	-0.243358+j0.275469

Table 3
Solutions of three-node system by Homotopy method

	E_1	E_1*	E_2	E_2*
	Power system solutions (E and E* are conjugate pairs)			
1	0.031675-j0.041027	0.031675+j0.041027	0.923969-j0.382479	0.923969+j0.382479
2	0.967058+j0.012747	0.967058-j0.012747	0.996533+j0.083196	0.996533-j0.083196
3	-0.005173-j0.238416	-0.005173+j0.238416	-0.489059-j0.872251	-0.489059+j0.872251
4	-0.009159-j0.107433	-0.009159+j0.107433	-0.238363-j0.971148	-0.238363+j0.971148
	None power system solutions (E and E* are not conjugate pairs)			
5	0.009447+j0.025249	0.364886+j1.672836	-0.735006-j0.177015	-1.285946+j0.309700
6	0.364886-j1.672837	0.009447-j0.025249	-1.285945-j0.309669	-0.735006+j0.177016

Table 4
Comparison of complex results by WEM and Homotopy method

	5		6	
	V_1	V_2	V_1	V_2
Wu	0.009447+j0.025250	-0.735007-j0.177015	0.364913-j1.672788	-1.285945-j0.309700
Homotopy	0.009447+j0.025249	-0.735006-j0.177015	0.364886-j1.672837	-1.285945-j0.309669
Difference	0+j0.000001	-0.000001+j0	0.000017+j0.00049	0-j0.000001

4.2 Analysis of Results

Set the digits as 50 when solving (p_1, p_2, p_3, p_4) by WEM. R_{51} in the CS is a polynomial with the only variable e_2, the highest order exponent being 40. So solve CS first to obtain the 40 groups of solutions. Back substitute all the 40 groups of solutions to

obtain the solutions of the original set. Table 2 shows all the 6 groups of solutions obtained by WEM, in which all the solutions are displayed in 6 digits for convenience.

Homotopy method is used to calculate power flow of the three-node system [10]. As shown in Table 3, there are 4 groups of power system solutions and 2 groups of non power system solutions. By comparing results in Table 2 and Table 3, the 4 groups of power system solutions are almost the same. As for the two groups of complex solutions in [10], the real part e and the imaginary part f of the voltage can not be separated from the results by Homotopy method. So add e and f obtained by WEM by the formula $V = e + jf$ to calculate V_1 and V_2. Table 4 shows the comparison of complex results by the two methods. By comparison, it can be concluded that the results obtained by WEM and Homotopy method are almost the same.

5 Plotting analytical $V-P$ and $V-Q$ curves

WEM can obtain all the solutions of power flow equations. Change the system operation condition to calculate the power flow by WEM while removing the complex results which do not satisfy the power system. Plot the analytical $V-P$ and $V-Q$ curves with all the results obtained by WEM. System operation stability can be analyzed through $V-P$ and $V-Q$ curves. The procedure of plotting the $V-P$ and $V-Q$ curves at PQ node in the three-node system is as follows.

The active and reactive power injections are negative at the PQ node in the three-node system. In the paper, the absolute values of the active and reactive powers are used for convenience to plot and explain.

In the three-node system, change P_1 with $Q_1 = 0.1$ to obtain all the power flow solutions to plot $V-P$ curve at node 1, as shown in Fig. 3. When P_1 is small, there are four groups of real solutions; as P_1 increases, two groups of the solutions tend to converge. When $P_1 = 0.278$, the upper branch and the lower branch of curve 2 converge at one point. As P_1 continues to increase, the remaining two groups of solutions also tend to converge. When $P_1 = 1.462$, the upper branch and the lower branch of curve 1 converge at one point. Curve 3 and curve 4 in Fig. 3 are the mean value of voltage (MVV) of curve 1 and curve 2, respectively, as changing P_1.

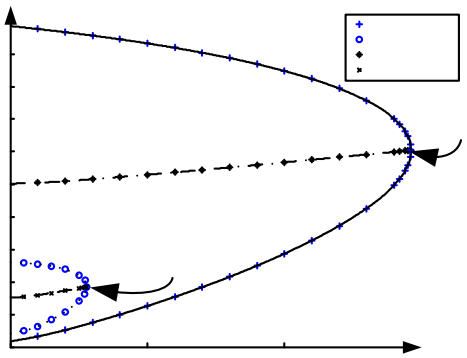

Fig. 3 $V-P$ curve with $Q_1 = 0.1$.

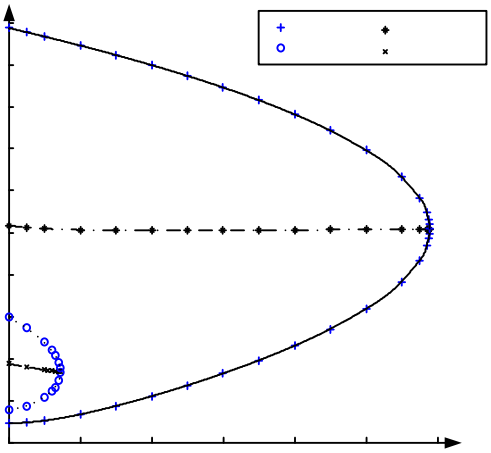

Fig. 4 $V-Q$ curves with $P_1 = 0.2$.

By analysis of $V-P$ curve in Fig. 3, the upper branches of curve 1 and curve 2 has similar changing trend. Further discussion should be made to make sure whether operational points in curve 2 are stable or unstable. The lower branches are clearly the unstable operation conditions.

In the three-node system, change Q_1 with $P_1 = 0.2$ to obtain all the power flow solutions to plot $V-Q$ curve at node 1, as shown in Fig. 4. The $V-Q$ curve is similar to $V-P$ curve. When $Q_1 = 0.1447$, the upper branch and the lower branch of curve 2 converge at one point. When $Q_1 = 1.178$, the upper branch and the lower branch of curve 1 converge at one point. Curve 3 and curve 4 in Fig. 4 are the MVV of curve 1 and curve 2 respectively as changing Q_1.

The fitting curves in Fig. 5 show the relationship between $Q_{\max}$ and $P_{\max}$ of operation limit conditions while $P > 0$, $Q > 0$. The shadow area A in Fig. 5 is the set of all the steady state operation conditions while the shadow area B is the set of

possible stable operation conditions with relatively high voltage under low voltage with light load.

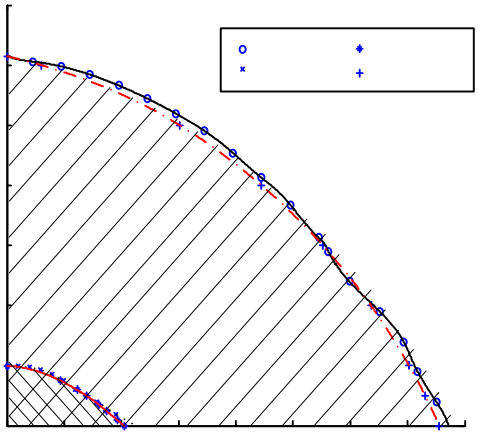

Fig. 5 Curves of $Q_{\max}$ - $P_{\max}$.

6 Properties of Jacobian matrix

The relationship between power and voltage as well as angle could be expressed in the linearized equations as follows:

$$\begin{bmatrix}\Delta P\\ \Delta Q\end{bmatrix}=\begin{bmatrix}J_{P\theta} & J_{PV}\\ J_{Q\theta} & J_{QV}\end{bmatrix}\begin{bmatrix}\Delta\theta\\ \Delta V\end{bmatrix}=J\begin{bmatrix}\Delta\theta\\ \Delta V\end{bmatrix} \quad (7)$$

where ΔP is the incremental change in bus active power; ΔQ is the incremental change in bus reactive power; $\Delta\theta$ is the incremental change in bus voltage angle; ΔV is the incremental change in bus voltage magnitude.

$J_R=[J_{QV}-J_{Q\theta}J_{P\theta}{}^{-1}J_{PV}]$ is the reduced Jacobian matrix.

By Schur's formula[19], we could obtain the following equation:

$$\det(J)=\det(J_{P\theta})\det(J_R) \quad (8)$$

The precondition of Schur formula is that $J_{P\theta}^{-1}$ exists. $J_{P\theta}$ is proved to be strictly invertable under general power system condition and an inreducible diagonally dominant matrix in [20]. As a result, Jacobian matrix J is singular when the reduced Jacobian matrix J_R is singular. The conclusion is to judge the voltage stability by Jacobian matrix or by the reduced Jacobian matrix using $V-Q$ sensitivity method are equivalent.

The rank of the Jacobian matrix for the three-node system is three. Keep reactive power constant while changing active power to calculate the operational parameters V_1, θ_1, θ_2. When P is small, there are four groups of solutions; when P is large, there are only two groups of solutions.

As shown in Table 5, when $P_1=0.27826$ (labeled as $P_{\max 1}$ with an arrow line in Fig. 3), $\det(J)$ corresponding to the two groups of solutions are almost zero; when $P_1=1.4622$ (labeled as $P_{\max 2}$ with an arrow line in Fig. 3), corresponding to the two remaining groups of solutions are almost zero. The first, second, third and fourth columns in Table 5, Table 6 and Table 7 are corresponding with the I, II, III, IV branches in Fig. 3, respectively.

$V-Q$ sensitivity analysis is used to measure the degree of system stability.

Let $\Delta P=0$, then $\Delta Q=J_R\Delta V$, where $J_R=[J_{QV}-J_{Q\theta}J_{P\theta}^{-1}J_{PV}]$. So $\Delta V=J_R^{-1}\Delta Q$. $J_R{}^{-1}$ is the reduced $V-Q$ Jacobian matrix in which i^{th} diagonal element is the $V-Q$ sensitivity at bus i. When $V-Q$ sensitivity is positive, the system is stable; the smaller the sensitivity, the more stable the system. Oppositely, when $V-Q$ sensitivity is negative, the system is unstable.

The J_R^{-1} of three-node system is first order matrix. So the $V-Q$ sensitivity equals the determinant of the matrix. The results are shown in Table 6 by which the degree of stability under different operation conditions can be measured.

Table 5

Determinant of Jacobian matrix with $Q_1=0.1$

P	1	2	3	4
0.1	49.523	-0.94215	0.26508	-0.58195
0.2	47.377	-0.68007	0.32121	-0.87177
0.2783	**45.58**	**-0.00193**	**0.00192**	**-1.1033**
0.4	42.581			-1.4355
0.8	30.908			-2.324
1.2	15.948			-3.2417
1.4	6.0196			-2.8313
1.4622	**0.026957**			**-0.02684**

As shown in Table 6, when $P>0.2782$, the number of the groups of solutions changes from 4 to 2; when $P>1.4622$, there is no solution of the power flow equations. The $V-Q$ sensitivities in the 1st and 2nd column are positive, so the system is stable. The $V-Q$ sensitivities in 3rd and 4th column are negative, so the system is unstable. The sensitivity is very large when reaching the stability limit. Even very small ΔQ would lead to large change of the voltage.

Table 7 shows the sign of $\det(J)$, $\det(J_{P\theta})$ and $\det(J_R)$ under different operational conditions in

Figure 3.

Analyze the changing process of $\det(J)$ first which is corresponding to operation conditions, as shown in curves 1 in Figure 3: $\det(J)>0$, corresponding to the upper branch of curve 1, as P increases; $\det(J)=0$, when P reaches the limit. In other words, J is singular; $\det(J)<0$, corresponding with the lower branch of curve 1. The changing process of $\det(J_R)$ is similar with that of $\det(J)$, while $\det(J_{P\theta})$ remains positive during the process.

The changing process of $\det(J)$ which is corresponding to operational conditions, as shown in curves 2 in Figure 3 is that: $\det(J)<0$, corresponding with the upper branch of curve 2, as P increases; $\det(J)=0$, when P reaches the limit. In other words, J is singular; $\det(J)>0$, corresponding with the lower branch of curve 2. The changing process of $-\det(J_R)$ is similar with that of $\det(J)$, while $\det(J_{P\theta})$ remains negative during the process.

Table 6
Determinant of reduced $V-Q$ Jacobian matrix with $Q_1=0.1$

P	1	2	3	4
0.1	0.20650	0.62638	-0.47230	-0.16627
0.2	0.20889	0.81873	-0.58465	-0.11176
0.2783	0.21113	**196.560**	**-196.300**	-0.09018
0.4	0.21539			-0.07315
0.8	0.24007			-0.0632
1.2	0.31740			-0.11914
1.4	0.54430			-0.34211
1.4622	**71.74**			**-71.522**

Table 7
The sign of $\det(J)$, $\det(J_{P\theta})$, and $\det(J_R)$ with $Q_1=0.1$

	1	2	3	4
$\det(J)$	+	−	+	−
$\det(J_{P\theta})$	+	−	−	+
$\det(J_R)$	+	+	−	−

By WEM, properties of Jacobian matrix are thoroughly analyzed above. The $V-Q$ sensitivities corresponding with the I and II branches in $V-P$ curve are positive. However, the properties shown in Table 5 and Table 7 are not the same, indicating different operational mode of power system.

7. Analysis of Equilibriums

Analysis in sections above focuses on static voltage stability. On basis of calculation, $V-P$ curve with four branches is obtained in section 5, showing that upper branches and lower branches with similar changing trend respectively. Through analysis of the Jacobian in section 6, further discussion should be made on these equilibriums.

Voltage stability and angle stability are two aspects of power system stability. The relationship between the two aspects is discussed [21]. A general energy function frame is presented for voltage and angle stability [22]. Since all the solutions of power flow equations could be obtained by WEM, it's convenient to analyze the operational mode of system. On the basis of the three-node system in Fig. 1, PV node connects with a generator denoted by a simple model compromising an internal voltage behind an effective reactance, as shown in Fig. 6. The results are denoted in polar coordinate form shown in Table 8, where V_g and θ_g represent the amplitude and angle of the internal voltage.

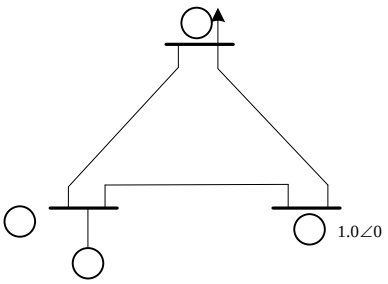

Fig. 6 Three-node system with a generator

Table 8
System equilibriums obtained by WEM

	V_1	θ_1/(°)	θ_2/(°)	V_g	θ_g/(°)
1	0.052	-52.3	-22.48	1.2774	-21.14
2	0.108	-94.8	-103.8	1.4527	-102.61
3	0.238	-91.2	-119.3	1.4564	-118.10
4	0.967	0.76	4.72	0.9989	6.49

Analysis of the relationship between voltage and angle stability is presented in [23], showing that the relationship could be linked by the unstable equilibrium points (UEP) which are classified into voltage stability mode with low voltage- small angle and angle stability mode with high voltage-large

angle. The first Equilibrium in Table 8 is voltage stability mode UEP, corresponding with point in IV branch in $V-P$ curve; the second equilibrium is with low bus voltage-large angle, corresponding with point in III branch in $V-P$ curve; the third equilibrium is angle stability mode UEP, corresponding with point in II branch in $V-P$ curve; the fourth equilibrium is the stable operational mode corresponding with point in I branch in $V-P$ curve.

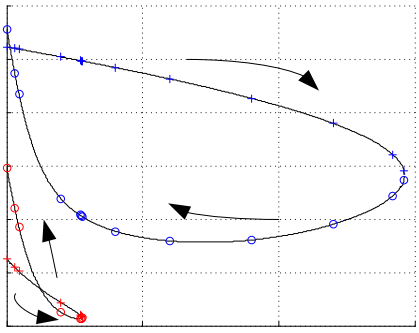

Fig. 7 $\theta_1 - P_1$ **curve**

Fig. 7 displays the locus curves of variation in the PQ bus angle with load. The arrows indicate the changing direction. The II branch is with large angle, corresponding with II branch in $V-P$ curve, indicating angle instability.

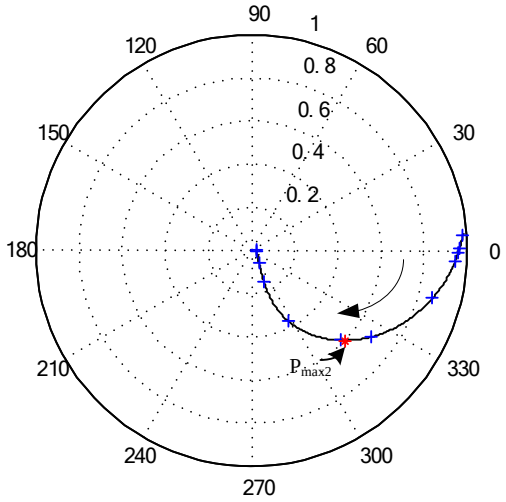

(a)

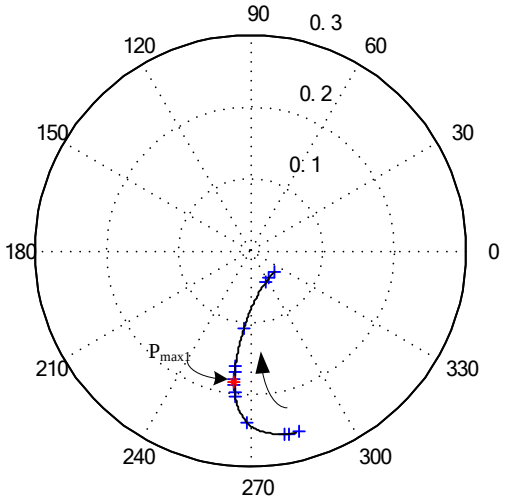

(b)

Fig. 8 $\theta_1 - V_1$ **curve in polar coordinates**

The $\theta_1 - V_1$ curves clearly show that the bus voltage decreases quickly after the bifurcation point denoted by an arrow line, while the bus voltage with large angle corresponding with the II branch in $V-P$ curve begins to decrease quickly before the bifurcation point.

Fig. 9 shows the variation in internal angle with the load. The equilibriums on the upper branch of curve 2 in $V-P$ curve are with large angle despite relatively high voltage, similarly with $\theta_1 - P_1$ curve.

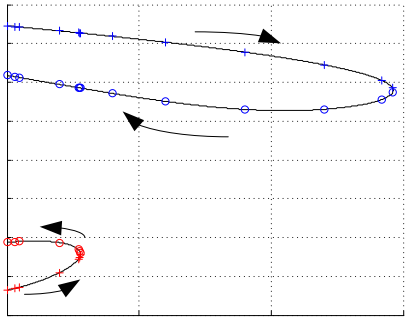

Fig. 9 $\theta_g - P_1$ **curve**

Fig. 10 display the variation in angular separation between buses of the three lines and inject active power with the load respectively, where $\theta_{21} = \theta_2 - \theta_1$ $\theta_{31} = \theta_3 - \theta_1$ $\theta_{32} = \theta_3 - \theta_2$ $\theta_3 = 0$ .The power directions are from bus 2 to bus 1, from bus 3 to bus 1, and from bus 3 to bus 1 respectively. In an idealized two-node model, the relationship between power and angle is sinusoidal. The variation in power with angular separation between buses of the three-node system is different from the sinusoidal relationship. However, valuable information could be obtained from the analysis of the relationship between power and angle.

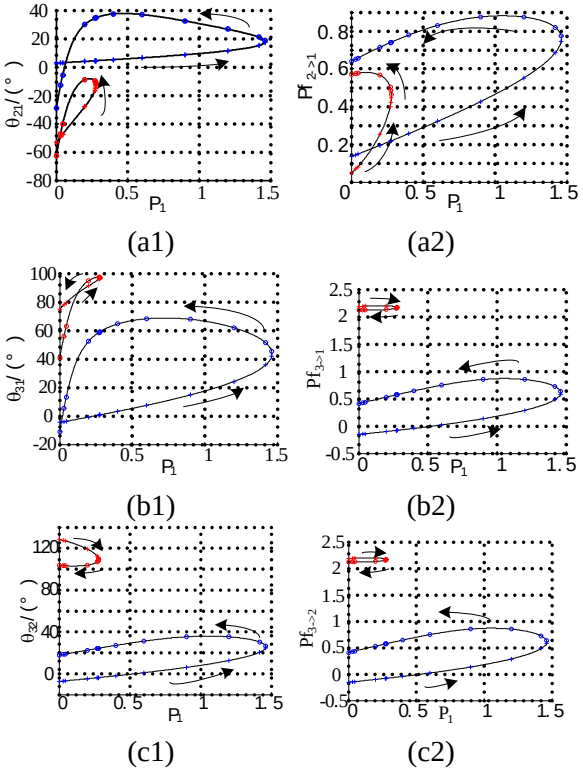

Fig.10 a1) $\theta_{21}-P_1$ **curve, a2)** $Pf_{21}-P_1$ **curve;**
b1) $\theta_{31}-P_1$ **curve, b2)** $Pf_{31}-P_1$ **curve;**
c1) $\theta_{32}-P_1$ **curve, c2)** $Pf_{32}-P_1$ **curve.**

Figures above show the locus of active power in each line of the three-node system with the change of the load. Table 9 shows the change trend of the active power in the three lines. The active power in the three lines increases with the load under operational mode corresponding with the I branch in $V-P$ curve, while there is "fluctuation" of active power in the lines under other operational mode corresponding to the other branches in $V-P$ curve.

Table 9
Change of active power in each line

	Curve 1		Curve 2	
	I branch	IV branch	II branch	III branch
Line 1-2	2→1↑	2→1↑↓	2→1↑	2→1↑↓
Line 2-3	2→3↓ 3→2↑	3→2↑↓	3→2↑↓	3→2↓↑
Line 1-3	1→3↓ 3→1↑	3→1↑↓	3→1↑↓	3→1↓↑

The practical power system is far more complex than the three-node system. However, the locus curves of operational parameters (e.g. the internal voltage of generation) could provide potentially valuable information for research on complex systems.

8. Conclusion

WEM can obtain all the analytical solutions of simultaneous polynomial equations without either extraneous roots or missing roots. As a result, WEM can solve power flow equations to plot analytical $V-P$, $V-Q$ curves as well as the steady operation area. The properties of power-flow Jacobian matrix are also analyzed, as well as testifying the properties of the active power/angle sub-matrix in the power flow Jacobian. Analysis of equilibriums is presented, showing that stable equilibrium point with high voltage-small angle, one UEP with low voltage-small angle, one UEP with high voltage-large angle, one UEP with low voltage-large angle. WEM provides a new way to study the characteristic of power system by obtaining all the solutions of power flow equations. However, it is difficult to solve the power flow equations by WEM when the number of nodes increases, for the exponent of variable in the equations are much high during the calculation procedure.

Acknowledgment

This work was supported by National Natural Science Foundation of China (69774003). The authors would like to thank Prof. Shi H. of Academy of Mathematics and System Science, Chinese Academy Science and Prof. Wang J. for their help.

References:

[1] Chen, C., Zhao, X.Q., and Cao, G.Y., Mechanized Mathematics–Wu Elimination Method Applied in Power System, *Proc. of the CSEE*, Vol. 18, No. 1, 1998, pp. 51-56.

[2] Chen, C., and Cao, W., The Application of Wu Method in Electric-magnetic Transient Analysis during Power System Short-circuit, *Proc. of the CSEE*, Vol. 22, No. 11, 2002, pp. 16-19.

[3] Jia, Y. F., Chen, Y. F., and Xu, Z. Q., Application of Wu Elimination Method to constrained Dynamics, *Applied Mathematics and Mechanics(English Edition)*, Vol. 27, No. 10, 2006, pp. 1399-1408.

[4] Wang, L.G., Hu, C., Huang, W. H., Application of Wu Elimination Method in Rotor Dynamics, *China Mechanical Engineering*, Vol. 13, No. 21, 2002, pp. 1805-1807.

[5] Tinney, W.F., and Hart, C.E., Power Flow Solution by Newton's Method, *IEEE Trans. on*

Power Apparatus and System, Vol. PAS-86, NO.11, 1967, pp. 1449-1460.

[6] Scott, B., and Alsac, O., Fast Decoupled Load Flow, *IEEE Trans. Power Apparatus and System*, Vol. PAS-93, No.3, 1974, pp. 859-869.

[7] KIos, A., and Kemer, A., The non-uniqueness of load flow solution, *Proc. of PSCC V*, 1975, pp. 3.1/8.

[8] Korsak, A. J., On the question of uniqueness of stable load-flow solutions, *IEEE Trans. on Power Apparatus and Systems*, Vol. PAS-91, No. 3, 1972, pp. 1093-1100.

[9] Salam, F. M. A. et al., Parallel processing for the load flow of power systems: the approach and applications, *Proc. of 28th IEEE Conf. on Decision and Control*, Vol. 3(13-15), 1989, pp.2173-2178.

[10] Guo, X.G., and Salam, F. M. A., The number of (equilibrium) steady-state solutions of models of power systems, *IEEE Trans. on Circuit and Systems*, Vol. 41, NO. 9, 1994, pp. 584-600.

[11] Ma, W., and Thorp, J. S., Solving for all the solutions of power systems equations, *Proc. 1992 IEEE ISCAS*, Vol. 5(3-6), 1992, pp. 2537-2540.

[12] Yin, X., Application of Genetic Algorithms to Multiple Load Flow Solution Problem in Electrical Power Systems, *Proceeding of the 32nd IEEE Conference on Decision and Control*, Vol. 4(15-17), 1991, pp. 3734-3739.

[13] Klump, R.P., Overbye, T.J., A new method for finding low-voltage power flow solutions, *IEEE Power Engineering Society Meeting*, Vol. 1 (16-20), 2000, pp. 593-597.

[14] Ai, Q, Gu, D., Jiang, C., et al, Research on propagation of voltage fluctuations along practical power distribution systems, *WSEAS Trans. on Circuits and Systems*, Vol. 4, No. 9, 2005, pp. 1136-1145.

[15] Gu, C., Ai, Q., Wu, J., Continuation power flow (CPF) and its usage in static voltage stability analysis considering different static load models and system operating constraints, *WSEAS Trans. on Circuits and Systems*, Vol. 4, No. 10,2005, pp.1395-1402.

[16] Li, H., Cheng, H., Wang, C., A novel approach for determining the Hopf bifurcation point of dynamic voltage stability in power system, *WSEAS Trans. On Circuits and System*, Vol. 4, No. 7, 2005, pp. 691-698.

[17] Wu, T. *Mathematics Mechanization*, Science Press/ Kluwer Pub., 2000.

[18] Wang, W. L., and Chen, C. Application of Wu Elimination Method in Solving for All the Steady-State Power Flow Solutions, *Journal of Shanghai Jiao Tong University*, Vol. 38, No. 8, 2004, pp. 1260-1264.

[19] Horn, R. A., and Zhang, F. *The Schur Complement and Its Application*, New York: Springer, 2005.

[20] Cao, G.Y., and Liu, L.X. Analysis on the Active Power/Angle Submatrix in Power Flow Jacobian Matrix, *Power System Technology*, Vol. 31, No. 15, 2007, pp. 50-54.

[21] Vournas C.D., Sauer P. W.. Relationships between Voltage and Angle Stability of Power System. *Electrical Power and Energy System*, Vol. 18, NO. 8, 1996, pp. 493-500.

[22] Overbye T. J., PaiM A., Sauer PW. Some Aspects of the Energy Function Approach to Angle and Voltage Stability Analysis in Power Systems. *Proceedings of the 31st Conference on Decision and Control Tucson (Artzons)*, 1992, pp. 2941-2946.

[23] WU H., HAN Z.. Analysis of the relationship between voltage stability and angle stability through equilibriums. *Automation of Electrical Power Systems*, Vol. 27, No. 12, 2003, pp. 28-311.